JOURNAL OF VIROLOGY, Oct. 2008, p. 10247–10261 Vol. 82, No. 20
0022-538X/08/$08.00+0 doi:10.1128/JVI.01035-08

The Vaccinia Virus Gene I2L Encodes a Membrane Protein with an Essential Role in Virion Entry▽

R. Jeremy Nichols,†§ Eleni Stanitsa,‡§ Bethany Unger, and Paula Traktman*

Department of Microbiology and Molecular Genetics, Medical College of Wisconsin, Milwaukee, Wisconsin 53226

Received 16 May 2008/Accepted 6 August 2008

The previously unstudied vaccinia virus gene I2L is conserved in all orthopoxviruses. We show here that the 8-kDa I2 protein is expressed at late times of infection, is tightly associated with membranes, and is encapsidated in mature virions. We have generated a recombinant virus in which I2 expression is dependent upon the inclusion of tetracycline in the culture medium. In the absence of I2, the biochemical events of the viral life cycle progress normally, and virion morphogenesis culminates in the production of mature virions. However, these virions show an ~400-fold reduction in specific infectivity due to an inability to enter target cells. Several proteins that have been previously identified as components of an essential entry/fusion complex are present at reduced levels in I2-deficient virions, although other membrane proteins, core proteins, and DNA are encapsidated at normal levels. A preliminary structure/function analysis of I2 has been performed using a transient complementation assay: the C-terminal hydrophobic domain is essential for protein stability, and several regions within the N-terminal hydrophilic domain are essential for biological competency. I2 is thus yet another component of the poxvirus virion that is essential for the complex process of entry into target cells.

Variola virus and vaccinia virus are perhaps the most notorious members of the poxvirus family: the former is the etiological agent of smallpox, and the latter has long been used as the vaccine to protect against smallpox. Poxviruses are the only DNA viruses whose life cycle is restricted to the cytoplasm of infected cells; the large repertoire of proteins encoded by the ~200-kb DNA genome of these viruses affords them a high degree of genetic and physical autonomy from host cells. The virions themselves are ~250 by 350 nm in size and contain ~75 proteins which localize to a delimiting and protein-rich membrane, two proteinaceous lateral bodies of unknown function, and a central core (9). The core, in addition to its numerous structural components, contains the viral genome and a transcriptional apparatus that is responsible for mediating early gene expression immediately after virion binding and entry. The binding of virions to target cells involves interactions between several virion membrane proteins (A27, D8, and H3) and glycosaminoglycans (GAGs) on the target cell (4, 5, 7, 21–23, 29) and is also presumed to involve higher-affinity interactions between as-yet-unidentified virion proteins and cellular receptors. Subsequent release of the virion core into the cytoplasm can occur either by direct fusion of the virion and plasma membranes or by engulfment of the intact virion followed by pH-dependent fusion events which result in the release of the core from the endocytic compartment and its deposition in the cytoplasm (4, 31, 51, 54).

Approximately 90 genes are conserved within the genomes of all chordopoxviruses and are therefore viewed as encoding the repertoire of proteins essential for completion of the viral life cycle (60). Through combined genetic, biochemical, and bioinformatic analyses, the roles played by the majority of the proteins encoded by these genes are being elucidated. As might be expected, these proteins collectively mediate virion entry, gene expression, genome replication and maturation, virion morphogenesis, and virion egress. However, a few of the gene products encoded by these 90 conserved genes remain unstudied. Among these, we chose the I2L gene for study because it was predicted to be expressed at late times of infection and to encode a small membrane protein. We therefore reasoned that it might be involved in the biogenesis of the virion membrane, an incompletely understood process which has been of historical interest to our laboratory.

We show here that the I2 protein is expressed at late times of infection, associates with membranes, and is present within mature virions. Moreover, we show that, when I2L is repressed, the biochemical progression of the life cycle and the process of virion morphogenesis are unaffected. However, the specific infectivity of the virions that are produced in the absence of the I2 protein is reduced ~400-fold because of their inability to enter target cells. Thus, I2 is an essential protein that plays a heretofore unknown role in the earliest stage of the infectious cycle.

MATERIALS AND METHODS

Materials, cells, and viruses. African green monkey kidney BSC40 cells, mouse L cells, and human thymidine kinase-negative (TK^-) 143B cells were cultured in Dulbecco's modified Eagle's medium containing 5% fetal calf serum (Invitrogen, Carlsbad, CA) at 37°C in the presence of 5% CO_2. Viral stocks were prepared by ultracentrifugation of cytoplasmic lysates through 36% sucrose; titration was performed on confluent monolayers of BSC40 cells, which were

* Corresponding author. Mailing address: Department of Microbiology and Molecular Genetics, Medical College of Wisconsin, 8701 Watertown Plank Rd., Milwaukee, WI 53226. Phone: (414) 456-8253. Fax: (414) 456-6535. E-mail: ptrakt@mcw.edu.

† Present address: MRC Protein Phosphorylation Unit, University of Dundee, Dundee, United Kingdom.

‡ Present address: McArdle Laboratory for Cancer Research, University of Wisconsin, Madison, WI 53706.

§ R.J.N. and E.S. contributed equally to this work.

▽ Published ahead of print on 13 August 2008.

TABLE 1. Oligonucleotide primers used in this study

Primer	Sequence[a]
HA-I2 1	5′-AT**GGATCC**GAATGCGTACTTCAGG-3′
HA-I2 B	5′-TTACGATGTCCCAGATTATGCAGATA AGTTGTA-3′
HA-I2 4	5′-AT**GGATCC**GGAGCCATGGTAG-3′
HA-I2 C	5′-AATCTGGGACATCGTAAGGGTACATT TATACAT-3′
I2 probe 5′	5′-ATGGATCCATTGATAGAGAAGTGG-3′
I2 probe 3′	5′-CCAACCCCAACAACCGG-3′
indI21	5′-GG**GGATCC***AAGCTT*ATGATGAAGATA GCG-3′
indI2-B	5′-CTCTATCACTGATAGGGATATTTATA CATTGAA-3′
indI2-C	5′-CCCTATCAGTGATAGAGAATGGATA AGTTGTAC-3′
indI2-4	5′-GGatcgatTCACCAAACAAC-3′
I1pucNeo A	5′-CCGCCG*ggtacc*GGTATTAAGAATTCG-3′
I1pucNeo B	5′-CG**GGATCC**GATATATTTGTATTTAAA AG-3′
I3pucNeo 5′	5′-CG<u>TCTAGA</u>TGGAGAATCATCCATTC-3′
I3pucNeo B/H 3′	5′-CG**GGATCC***AAGCTT*TTATACATTGAAT ATTG-3′
I2-5′	5′-CCatcgatGGATAAGTTGTACGCC-3′
I2-3′	5′-GC**GGATCC**TCACCAAACAACTTTTA-3′
Δ1-12 5′	5′-CCatcgatGGGGTCTCCGGAAG-3′
EDD-AAA5′	5′-GGGGTCTCCGGCTGCTGCTTTGACAG ACTTTAT-3′
EDD-AAA3′	5′-GTCTGTCAAAGCAGCAGCCGGAGAC CCC-3′
DK-AA-5′	5′-CCatcgatGGCTGCGTTGTACGCCGC-3′
Tet^{r}5′	5′-CAGCGCATTAGAGCTC-3′
Tet^{r}3′	5′-TTAAGACCCACTTTCACA-3′
YFF-AAA-5′	5′-CCatcgatGGATAAGTTGGCCGCCGCTA TAGCTGGTGTAGCTA TGGGGTCTCC G-3′
FI-AA 5′	5′-TGACAGACGCTGCAGAAATTGTTAA ATC-3′
FI-AA 3′	5′-CAATTTCTGCAGCGTCTGTCAAATC-3′
DEK-AAA 5′	5′-TTCTAAGTGCTGCGGCAACAGTCACA TC-3′
DEK-AAA 3′	5′-GTGACTGTTGCCGCAGCACTTAGAAC AG-3′
I2-path 5′	5′-at**gaattc**atggataagttgtacg-3′
I2-path 3′	5′-ccatcgatttaaccccaacaacc-3′
I2-pTM1/pUC1246 5′	5′-ta**ggatcc**catatggataagttgtac-3′
I2-pTM1/pUC1246 3′	5′-GC**GGATCC**TCACCAAACAACTTTTA-3′

[a] Restriction enzyme sites contained in primers are indicated as follows: BamHI, boldface; HindIII, italic; ClaI, lowercase; Asp718, lowercase italic; EcoRI, lowercase boldface; XbaI, small caps; NdeI, underlined.

fixed and stained with 0.1% crystal violet in 3.7% formaldehyde at 48 postinfection (hpi). Restriction endonucleases, T4 DNA ligase, calf intestinal alkaline phosphatase (CIP), and *Taq* polymerase were purchased from Roche Applied Sciences (Indianapolis, IN). Geneticin (G418 sulfate), Lipofectamine 2000, protein molecular weight markers, DNA molecular weight standards, and Texas Red-phalloidin were purchased from Invitrogen (Carlsbad, CA). ^{14}C-labeled protein molecular weight standards were obtained from Amersham/GE Life Sciences (Piscataway, NJ). $^{32}P_i$ and [^{35}S]methionine were purchased from Perkin-Elmer Life and Analytical Sciences, Inc. (Boston, MA). Ultrapure chemicals, protein A-Sepharose, and protein G-agarose were from Sigma Aldrich (St. Louis, MO). DNA oligonucleotides were synthesized by IDT (Coralville, IA). Monoclonal hemagglutinin (HA) antibody was acquired from Covance Research Products (Princeton, NJ). Antibodies to the A21, A28, and G3 proteins were kindly supplied by B. Moss (NIAID, NIH, Bethesda, MD). The antibody to the A5 protein was kindly supplied by M. Esteban (Centro Nacional de Biotecnología, Madrid, Spain).

Plasmid and recombinant virus construction. The primers used to amplify wild-type, epitope-tagged, and mutant alleles of I2 used in the generation of plasmids and viruses described in this work are shown in Table 1.

Construction of vHA-I2, which encodes an HA-tagged I2 allele within the endogenous I2L locus. (i) Preparation of pUCneo-I1-HA-I2-I3. A cassette comprising the 3′ 346 bp of I1, the I2 promoter, the I2 open reading frame (ORF) in which 27 bp encoding the 9-amino-acid (aa) HA epitope was inserted immediately after the initiating ATG codon, and the 5′ 288 bp of the I3L ORF was prepared by overlap PCR using viral genomic DNA as a template. Two initial PCRs were performed using HAI2 1 plus HAI2 B and HAI2 C plus HAI2 4. The products derived from these two reactions overlapped by 17 bp and were combined and used as the templates for a second round of PCR performed with the outside primers HA-I2 1 and HA-I2 4. The PCR product generated was digested with BamHI and ligated with pUCneo (16) plasmid that had been previously digested with BamHI and treated with CIP.

(ii) Transient dominant selection: generation of vHA-I2. Confluent 35-mm dishes of BSC40 cells were infected with wild-type (wt) virus (multiplicity of infection [MOI] of 0.03) and transfected with 5 μg of supercoiled pUCneo-I1-HA-I2-I3 plasmid DNA at 3 hpi with Lipofectamine 2000. At 16 hpi, G418 was added to 3 mg/ml to select for viruses in which the pUCneo-I1-HA-I2-I3 plasmid had integrated into the viral genome. At 48 hpi, cells were harvested and G418^r viruses were isolated by two rounds of plaque purification in the presence of G418. PCR was performed with primers specific for the neomycin resistance (Neo^r) cassette (NEO) to confirm plasmid integration (16). G418^r viruses were subjected to sequential rounds of plaque purification in the absence of drug, allowing for recombination between the tandem repeats of sequences derived from the I1L, I2L, and I3L genes that are present in this intermediate virus. To distinguish viruses containing only the wt allele from those containing the HA-tagged targeted locus, plaque isolates were screened by PCR using primers that flank the I1 3′ and I2 5′ junction (I2 probe 5′ and I2 probe 3′) and generate products of 248 or 221 bp that correspond to the targeted or wt locus, respectively.

Construction of vΔ*ind*I2. To enable inducible expression of the protein I2, we generated vΔ*ind*I2, in which an inducible copy of the I2 gene has been placed within the TK locus and the endogenous I2 gene has been deleted.

(i) Construction of pJS4:tetR↔ indI2. The pJS4:tetR plasmid (59), based on the pJS4 plasmid (gift of B. Moss, NIH), contains two divergent promoters: one driving constitutive expression of the tetracycline (TET) repressor (tetR) and the other preceding a multicloning site. These two cassettes are flanked by the left and right halves of the TK gene, which enables their insertion into the genome by homologous recombination. The second promoter region was replaced with a fragment representing a TET-regulated copy of the I2 gene under the control of the endogenous I2 promoter. Overlap PCR was used to generate a 281-bp fragment containing the 222-bp I2L ORF, the 19-bp Tet operator sequence, and 40 bp of upstream sequence containing the I2 promoter. Using vaccinia virus genomic DNA as template, PCRs were performed using primers indI2-1 plus indI2-B and indI2-C plus indI2-4; the products of these reactions overlapped by 17 bp and were used together as the template for a second round of PCR performed with primers indI2-1 and indI2-4. The final PCR product was digested with ClaI and HindIII and ligated to pJS4:tetR DNA that had been similarly digested. Plasmids containing the fragments in the appropriate orientation were identified by restriction enzyme analysis; the final plasmid was designated pJS4:tetR↔ *ind*I2.

(ii) Intermediate virus construction. To achieve insertion of the tetR-inducible I2 cassette into the TK locus, cells were infected with wt virus (MOI of 0.03) and transfected with linearized pJS4:tetR↔ indI2 DNA at 3 hpi. At 48 hpi, the cells were harvested and TK$^-$ virus was isolated by two rounds of plaque purification on human TK$^-$ cells in the presence of 25 μg/ml bromodeoxyuridine. Insertion of the cassette was confirmed by PCR using primers directed to the tetR sequence (Tet^{r}5′ and Tet^{r}3′) (56). Plaques of the correct genotype were expanded, and this virus was designated v*ind*I2.

(iii) Generation of the final vΔ*ind*I2 virus. Once the inducible I2 gene had been inserted into the TK locus, the final step required for the generation of the inducible virus was the replacement of the endogenous I2 allele with NEO.

(a) Generation of the pI2KO vector. PCRs were performed with primers I1pucNeo A and I1pucNeo B, which enabled the amplification of a 300-bp I1L fragment containing Asp718 and BamHI sites at the 5′ and 3′ termini, respectively. Primers I3pucNeo B/H and I3pucNeo 5′ were used to amplify a 324-bp I3L fragment containing BamHI/HindIII and XbaI sites at the termini. The I1L fragment was digested with Asp718 and BamHI, and the I3L fragment was digested with BamHI and XbaI. These products were ligated simultaneously to pBSIIKS vector DNA (Stratagene; La Jolla, CA) that had been previously digested with Asp718 and XbaI and treated with CIP. The resultant plasmid, pBSIIKS-I1-I3, was then used for the next round of cloning. A 1.3-kb fragment containing the Neo^r gene under the regulation of a constitutive viral promoter was released from pUCneo (16) by digestion with BamHI and HindIII, and the 5′ overhangs were filled in with the Klenow fragment of *Escherichia coli* DNA polymerase. The plasmid pBSIIKS-I1-I3 was linearized at the internal BamHI site and treated with CIP, and the 5′ overhangs were similarly filled. This linearized plasmid was then ligated with the NEO gene; the resulting plasmid, which contained portions of the I1 and I3 genes flanking NEO, was designated pI2KO.

***(b) Generation of* v*Δind*I2.** Cells were infected with v*ind*I2 at an MOI of 0.03 and transfected with linearized pI2KO DNA. G418 was added at 15 hpi; cells were harvested at 48 hpi, and $G418^r$ viruses were isolated by two rounds of plaque purification in the presence of G418 (3 mg/ml) and TET (1 μg/ml). The final virus, in which the endogenous allele had been replaced with NEO and the inducible allele was inserted within the TK locus, was designated v*Δind*I2.

Transient complementation assay. (i) Construction of pUC1246 constructs. The I2 ORF, or variants thereof, was amplified from vaccinia virus genomic DNA by PCR using the primers indicated below. PCR products were digested with ClaI and BamHI and ligated with pUC1246 vector (56) that had been digested similarly and treated with CIP. (i) To generate pUC1246-I2Δ1–12, a single PCR was performed using primers Δ1-12-5′ and I2-3′. (ii) To generate pUC1246-I2-DK, primers DK-AA-5′ and I2-3′ were used. (iii) To generate pUC1246-I2-EDD, primer pairs EDD-AAA5′ with I2-3′, and I2-5′ with EDD-AAA3′ were used for the initial rounds of PCR. The products were used as templates for a second round of PCR with the outside I2-5′ and I2-3′ primers. (iv) To generate pUC1246-I2-DEK, primer pairs DEK-AAA 5′ with I2-3′ and I2-5′ with DEK-AAA 3′ were used for the first round of PCR. The products were used as templates for overlap PCR using the outside I2-5′ and I2-3′ primers. (v) To generate pUC1246-I2-FI, primer pairs FI-AA 5′ with I2-3′, and I2-5′ with FI-AA 3′ were used for the first round of PCR. The products were used as templates for overlap PCR using the outside I2-5′ and I2-3′ primers. (vi) Generation of pUC1246-I2-YFF was performed with primers YFF-AAA-5′ and I2-3′.

(ii) Transient complementation. Confluent 35-mm dishes of BSC40 cells were infected with v*Δind*I2 (MOI of 3) in the presence (+) or absence (−) of TET. At 3 hpi, cells infected in the absence of TET were either left alone or transfected with 4 μg of the indicated plasmid using Lipofectamine 2000. At 24 hpi, cells were harvested and the yield of infectious virus was determined by titration on BSC40 cells. Accumulation of the transiently expressed protein within the infected/transfected cells was assessed by immunoblot analysis using the anti-I2 serum.

Generation of a polyclonal anti-I2 antiserum. (i) Construction of pATH11-I2ΔC′. To prepare a recombinant immunogen, we constructed a plasmid encoding a trpE-I2 fusion protein which incorporated the hydrophilic portion of I2. Sequences encoding the N-terminal 47 aa of I2 were amplified using vaccinia virus genomic DNA as a template and primers I2-path 5′ and I2-path 3′. The 141-bp PCR product was digested with EcoRI and ClaI and then ligated with pATH11 vector (27) that had been similarly digested and treated with CIP. The resulting plasmid was designated pATH11-I2ΔC′.

(ii) Expression and isolation of trpE-I2ΔC′. *E. coli* strain HB101 transformants harboring pATH11-I2ΔC′ were induced to express the 41-kDa fusion protein. Cells were lysed, and the insoluble fraction was resolved by sodium dodecyl sulfate-polyacrylamide gel electrophoresis (SDS-PAGE); the trpE-I2ΔC′ fusion protein was visualized by copper staining, and the excised gel slice was used as an immunogen in rabbits. Antigen injection and serum procurement were performed by PRFAL (Canadensis, PA).

Construction of pTM-3XFLAG-I2 and pUC1246-I2. The 222-bp I2 ORF was amplified using viral genomic DNA as a template and the I2-pTM1/pUC1246 5′ and I2-pTM1/pUC1246 3′ primers. These primers inserted terminal NdeI site or BamHI sites, which were used to ligate the insert into pTM1-3XFLAG or pUC1246 vectors (32, 39, 56) that had been similarly digested and treated with CIP.

Subcellular fractionation by alkaline sodium carbonate extraction. Confluent 60-mm dishes of BSC40 cells were infected with vTF7-3 or wt vaccinia virus. At 3 hpi, cells were transfected with 10 μg of pTM1-3XFLAG-I2 (vTF7-3 infection) or pUC1246-I2 (wt infection). Cell pellets prepared at 18 hpi were washed with 10 mM Tris (pH 7.4) and 100 mM NaCl and collected by centrifugation. The resulting cell pellets were resuspended in cold 100 mM Na_2CO_3 (pH 11.5) and disrupted with a Dounce homogenizer. Lysates were incubated on ice for 30 min and then sedimented at 150,000 × *g* for 30 min. The membrane pellet was resuspended in an equal volume of 100 mM Na_2CO_3. The supernatant and pellet fractions were acetone precipitated and then resuspended in equal volumes of protein sample buffer.

Immunoblot analysis. Proteins were resolved on SDS-polyacrylamide gels and transferred to nitrocellulose (Schleicher & Schuell, Keene, NH) in CAPS buffer [10 mM 3-(cyclohexylamino)-1-propanesulfonic acid, 10% methanol (pH 11.3)]. Filters were probed with primary antisera followed by the appropriate horseradish peroxidase-conjugated anti-rabbit or anti-mouse secondary antibodies. After development with the West Pico enhanced chemiluminescent reagent (Pierce, Rockford, IL), immunoreactive proteins were visualized using Kodak MR film or an Alpha Innotec FluorChem 8800 documentation system.

Immunoprecipitation analysis. Confluent monolayers of BSC40 cells were infected with the appropriate virus and metabolically labeled with [^{35}S]methionine for the indicated times; cytosine arabinoside (AraC) was included in the culture medium at 20 μM where indicated. Cells were lysed in phospholysis buffer (10 mM $NaPO_4$ [pH 7.4], 100 mM NaCl, 1% Triton X-100, 0.1% SDS, 0.5% sodium deoxycholate), and clarified lysates were incubated with antibody for 4 h on ice followed by the addition of protein A or G for 1.5 h. Immune complexes were washed twice in lysis buffer and analyzed by SDS-PAGE. Gels were visualized by autoradiography using a Kodak low-emission screen.

Virion purification and fractionation. (i) Virion purification. BSC40 cells were infected with the virus of interest at an MOI of 2. At 24 hpi, cells were harvested and purified virions were purified from cytoplasmic lysates by ultracentrifugation through 36% sucrose followed by banding on 25 to 40% sucrose gradients. Virions were quantitated by determining the optical density (OD), using the conversion factor of 1 OD at 260 nm (OD_{260}) unit = 1.2×10^{10} virion particles per ml. Infectious viral yield was determined by titration on BSC40 cells.

(ii) Virion fractionation. Banded virions were incubated at 37°C for 30 min in one of the following reaction mixtures: 100 mM Tris (pH 9.0), 100 mM Tris (pH 9.0) with 0.1% NP-40 (vol/vol), or 100 mM Tris (pH 9.0) with 0.1% NP-40 (vol/vol) and 50 mM dithiothreitol (DTT). Soluble and particulate fractions, representing the membrane and core components of the virion, were partitioned by sedimentation (16,000 × *g* for 30 min at room temperature) and analyzed by immunoblot analysis with an anti-HA monoclonal antibody and antisera recognizing representative proteins of the virion membrane and core.

Analysis of viral protein synthesis and proteolytic processing of virion proteins. (i) Protein synthesis. Confluent 35-mm dishes of BSC40 cells were infected with v*Δind*I2 at an MOI of 10 in the presence or absence of inducer. At 2, 4, 6, and 8 hpi, cells were rinsed with methionine-free medium (DME-met) and pulsed for 30 min with DME-met containing 100 μCi/ml [^{35}S]methionine.

(ii) Proteolytic processing. Confluent 35-mm dishes of BSC40 cells were infected with v*Δind*I2 at an MOI of 10, in the presence or absence of inducer. As a control, a parallel sample was infected with wt virus in the presence of rifampin (RIF [100 μg/ml]) for the duration of the experiment. At 8 hpi, cells were rinsed with DME-met and pulsed for 30 min in DME-met containing 100 μCi/ml [^{35}S]methionine. Cells were either harvested immediately as described above (pulse) or fed with DME plus 5% fetal bovine serum (FBS) (containing methionine) and harvested at 24 hpi (chase). For both the time course and the analysis of protein processing, samples were fractionated on 10 to 17% SDS-polyacrylamide gels and visualized by autoradiography.

Analysis of DNA content of purified virions. Equal amounts of purified v*Δind*I2 ± TET or vTetR viral particles were diluted in 50 μl of water, boiled for 5 min, and applied (using a Bio-Dot microfiltration apparatus [Bio-Rad]) to a hydrated ZetaProbe membrane (Bio-Rad). Samples were denatured and renatured in situ, and the blot was then subjected to Southern dot blot hybridization using 10^6 cpm/ml of a radiolabeled probe representing the vaccinia virus HindIII E and HindIII F genomic fragments (20, 55). The levels of hybridized probe were visualized and quantitated by autoradiography and phosphorimager analysis.

Acid-induced "fusion from without." Confluent monolayers of BSC40 cells were placed on ice for 15 min in the presence of 300 μg/ml cycloheximide, which was present in all further steps. Cells were inoculated in duplicate with 10,000 particles/cell of purified $I2^+$ or $I2^-$ virions and maintained for 1 h on ice. Cells were then washed three times with phosphate-buffered saline (PBS) and pulsed with neutral fusion buffer (PBS with 10 mM MES [morpholineethanesulfonic acid]and 10 mM HEPES [pH 7.4]) or acidic fusion buffer (PBS with 10 mM MES and 10 mM HEPES [pH 5.5]) for 2 min at 37°C. Cells were then fed with Dulbecco's modified Eagle's medium plus 5% FBS (with cycloheximide) and incubated at 37°C for 3 h. Phase-contrast pictures were captured with a Nikon Coolpix camera.

Immunofluorescence. (i) Visualization of actin tails. BSC40 cells were infected at an MOI of 2 for ~18 h and then fixed for 15 min at room temperature in 4% paraformaldehyde–4% sucrose–PBS. Texas Red-phalloidin was used to stain actin, and DAPI (4′,6′-diamidino-2-phenylindole dihydrochloride) was used to detect DNA.

(ii) Virion binding and entry. BSC40 cells were grown to confluence in four-well chamber slides and chilled on ice for 10 min prior to infection with 300 particles/cell of purified $I2^+$ or $I2^-$ virions. After 1 h, the "no-shift" samples were washed with PBS and fixed with 4% paraformaldehyde in PBS (20 min on ice). "Shifted" samples were washed with PBS containing 300 μg/ml cycloheximide, fed with prewarmed media containing 5% FBS and 300 μg/ml cycloheximide, and incubated at 37°C for 1.5 h before being fixed. Fixed cells were then quenched, permeabilized, and blocked prior to incubation with anti-A17 or anti-39-kDa protein (A5) (generously provided by M. Esteban) sera followed by the appropriate fluorescent-conjugated secondary antibodies (Molecular

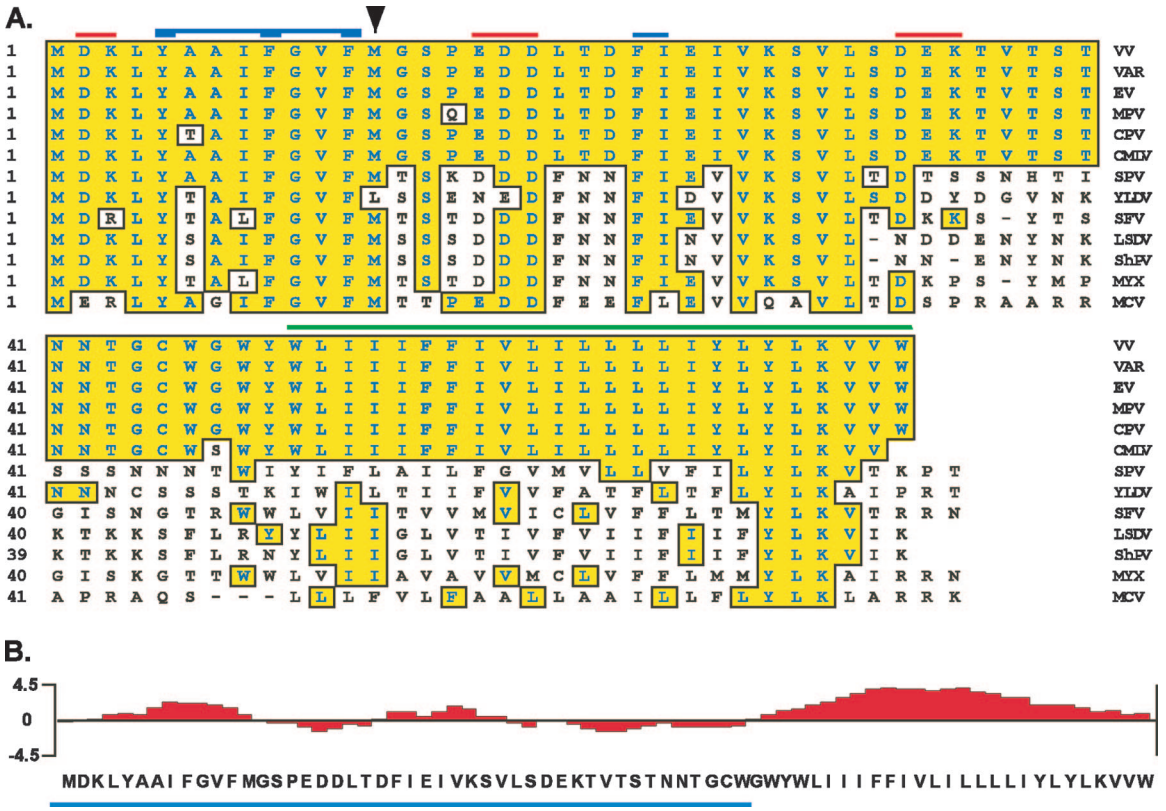

FIG. 1. Conservation and structural organization of the I2 protein. (A) Sequence alignment of the poxviral I2 homologs. Shown is a sequence alignment of the I2 orthologs from vaccinia virus (WR strain) (VV [GenBank identification no. 29692238]), variola virus (VAR [GenBank no. 439035]), ectromelia virus (EV [GenBank no. 22164721]), monkeypox virus (MPV [GenBank no. 179750543]), cowpox virus (CPV [GenBank no. 20178507]), camelpox virus (CMLV [GenBank no. 18640364]), swinepox virus (SPV [GenBank no. 18640187]), Yaba-like disease virus (YLDV [GenBank no. 12085087]), swine fever virus (SFV [GenBank no. 18448493]), lumpy skin disease virus (LSDV [GenBank no. 151505037]), sheeppox virus (ShPV [GenBank no. 21492557]), myxoma virus (MYX [GenBank no. 18426922]), and molluscum contagiosum virus (MCV [GenBank no. 1492060]). (Sequences were obtained from www.poxvirus.org by using the POCs program.) Residues identical to vaccinia virus I2 are boxed and shaded in yellow; the green line marks a predicted membrane-anchoring domain, and the red and blue lines and arrowhead refer to residues chosen for mutagenesis. (B) Hydrophobicity plot of the I2 protein. The C terminus of I2 is predicted to contain a transmembrane domain (aa 47 to 73 [green line in panel A]). The region marked by the blue line was used to generate the anti-I2 serum.

Probes). DAPI was applied to visualize DNA. Images were taken on a Nikon Eclipse TE 2000-U microscope using a Photometrics Cool Snap EZ camera and Metamorph software. The images shown were selected from a z-series that had been subjected to deconvolution using a nearest-neighbor format.

Electron microscopy. Confluent 60-mm dishes of BSC40 cells were infected with vΔ*ind*I2 in the presence or absence of inducer. At 17 hpi, cells were fixed in situ with 1% glutaraldehyde in PBS for 1 h on ice and processed for conventional transmission electron microscopy. Samples were examined on a Hitachi H-600 electron microscope.

Computer analysis. DNA and amino acid sequences of I2 poxvirus orthologs were retrieved from www.poxvirus.org. Sequence analyses were carried out with LaserGene software (DNASTAR, Madison, WI); amino acid alignments were performed using ClustalW. Autoradiographic films and electron microscopy negatives were scanned with an Epson 2400 scanner, adjusted in Adobe Photoshop (Adobe Systems, Inc., San Jose, CA) or Canvas 8.0 (Deneba Systems, Miami, FL), and figures were labeled with Canvas 8.0.

RESULTS

The goal of this work was to analyze the structure and function of the previously uncharacterized protein encoded by the vaccinia virus I2L ORF. I2L is predicted to encode a 72-aa protein with a calculated molecular weight of 8,400. Figure 1A presents a ClustalW multiple-sequence alignment of the amino acid sequence of the I2 proteins encoded by diverse chordopoxviruses. The first 33 aa of the protein are highly conserved; the aromatic/nonpolar and charged residues marked with the blue and red lines, respectively, were chosen for mutagenesis studies that will be described later in this report. The arrowhead represents the start of an N-terminal truncation mutant which was also analyzed. Each of the orthologs possesses a region of extreme hydrophobic character that begins at residue 48, as indicated by the green line; this region is predicted to be a C-terminal membrane-anchoring domain. This domain is easily seen in Fig. 1B, which represents a Kyte-Doolittle hydrophobicity plot. The blue bar in Fig. 1B indicates the portion of the protein used for preparation of the anti-I2 antiserum.

The I2 protein is expressed at late times of infection, associated with membranes, and incorporated into virions. The anti-I2 antibody that we generated showed good specificity and was useful in some analyses of the endogenous I2 protein, but there were assays in which detection of the endogenous protein with this antibody proved difficult. We therefore found it efficacious to construct a recombinant virus that expressed an N-terminally HA-epitope-tagged I2 protein from the endoge-

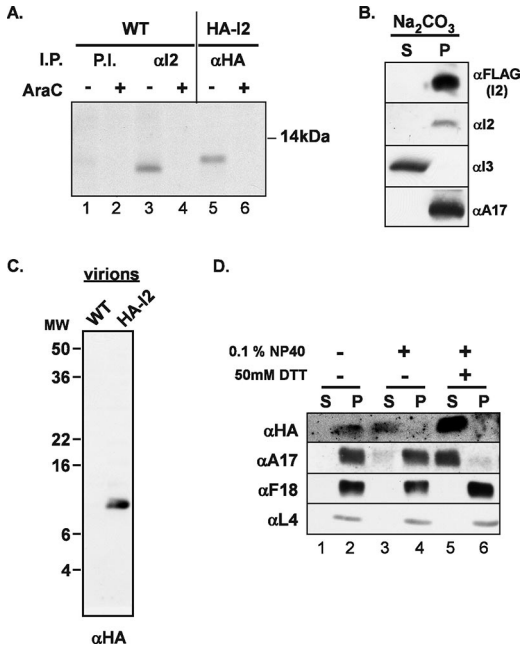

FIG. 2. I2 is a late protein that associates with membranes and is present within purified virions. (A) I2 is a late protein. Cells were infected with wt virus (lanes 1 to 4) or vHA-I2 (lanes 5 and 6) in the presence (lanes 2, 4, and 6) or absence (lanes 1, 3, and 5) of AraC and were metabolically labeled with [^{35}S]Met from 3 to 8 hpi. Lysates were subject to immunoprecipitation (I.P.) analysis with preimmune (P.I. [lanes 1 and 2]), anti-I2 (αI2 [lanes 3 and 4]), or anti-HA (αHA [lanes 5 and 6]) antibodies. (B) I2 is a membrane protein. Cells infected with wt virus were transfected with pUC1246-I2, while cells infected with vTF7-3 were transfected with pTM13XFLAG-I2, so as to express wt I2 or 3× FLAG-tagged I2, respectively. Cells were harvested at 18 hpi and subjected to Na_2CO_3 fractionation; the supernatant (S) and pellet (P [membranes]) fractions were subjected to immunoblot analysis using anti-FLAG, anti-I2, anti-I3, or anti-A17 antibodies (αFLAG, αI2, αI3, and αA17, respectively), as indicated. (C) Encapsidation of I2 protein. Ten micrograms of purified wt and vHA-I2 virions was resolved by SDS–17% PAGE and subjected to immunoblot analysis with an anti-HA antibody. (D) Subvirion fractionation. To determine the localization of I2 within virions, 2 μg of purified HA-I2 virions was treated with buffer (lanes 1 and 2) or with NP-40, either alone (lanes 3 and 4) or in the presence of DTT (lanes 5 and 6); the soluble (S [lanes 1, 3, and 5]) and pellet (P [lanes 2, 4, and 6]) fractions were resolved by sedimentation and subjected to immunoblot analysis using anti-HA, anti-A17, anti-F18 (αF18), and anti-L4 (αL4) sera.

nous locus (vHA-I2). The growth properties of this virus were indistinguishable from those of wt virus (not shown). To examine the temporal profile of I2 expression, cells were infected with wt or vHA-I2, in either the presence or absence of cytosine arabinoside (AraC), and were metabolically labeled with [^{35}S]methionine from 3 to 8 hpi. Cell lysates were subjected to immunoprecipitation with preimmune serum (Fig. 2, lanes 1 and 2) or anti-I2 (lanes 3 and 4) or anti-HA (lanes 5 and 6) serum. A labeled protein of ~8.4 kDa (from the wt infections) or ~8.7 kDa (from vHA-I2 infections) was immunoprecipitated by the anti-I2 and anti-HA antibodies, respectively. I2 was not found in samples prepared from cells infected in the presence of AraC, indicating that I2 is an intermediate or late protein whose expression is induced following the onset of viral DNA replication.

Sodium carbonate treatment is an efficient means of partitioning integral or lipid-anchored proteins that are tightly associated with membranes away from extrinsic membrane proteins (18). To monitor the predicted association of I2 with membranes, sodium carbonate fractionation was therefore performed on cells infected with wt virus or vTF7-3 (expresses the T7 polymerase) (14, 17). The wt virus-infected cells were transfected with pUC1246-I2, and vTF7-3 infected cells were transfected with pTM13XFLAG-I2. The pellet and soluble fractions were separated by ultracentrifugation and subjected to immunoblot analysis using anti-FLAG, anti-I2, anti-I3, or anti-A17 antibodies (Fig. 2B). I2 and 3XFLAG-I2 were found exclusively in the pellet, along with a known membrane component, A17 (43, 45, 64). As expected, the single-stranded DNA binding protein I3 (42) was found in the soluble fraction. To address whether I2 is encapsidated in mature virions, virions purified from wt and vHA-I2 infections were subjected to immunoblot analysis with monoclonal anti-HA antibody. As shown in Fig. 2C, the HA-I2 protein is indeed encapsidated. Furthermore, the subvirion localization of I2 was assessed by treating virions with NP-40 in the absence or presence of DTT. The membrane (soluble) and core (pellet) fractions were separated by sedimentation and analyzed by immunoblot analysis (Fig. 2D). Treatment of HA-I2 virions with NP-40 was sufficient to release the I2 from the virion into the soluble fraction, whereas release of A17 required treatment with both NP-40 and DTT, as we have observed before (32). As expected, the F18 and L4 proteins remained in the core fraction (pellet) after both treatments. Cumulatively, these data show that I2 is expressed at late times of infection and is a component of the virion membrane that can be extracted with detergent alone.

I2 is essential for plaque formation and for production of infectious virus from a single infectious cycle. The high degree of conservation of the I2 ORF in diverse poxviruses suggested that it might play an important role in the viral life cycle. To test this possibility, we constructed a recombinant vaccinia virus in which expression of I2 is regulated by the TET operator/repressor system (vΔ*ind*I2). The inducible copy of I2 and the TetR gene were inserted into the nonessential TK locus of the genome, and the endogenous I2 allele was replaced by NEO. A schematic representation of the relevant regions of the genome of this recombinant virus is shown in Fig. 3A. As shown in Fig. 3B, plaque formation by vΔ*ind*I2, but not by the parental vTetR virus (in which the TET repressor gene alone has been inserted into the TK locus), is dependent on the presence of the TET in the medium. Because the plaque assay measures both the production and spread of infectious virus, we also performed a quantitative assessment of the 24-h viral yield from vTetR and vΔ*ind*I2 infections (MOI of 2) performed in the presence or absence of TET. Although equivalent viral yields were obtained from cells infected with vTetR ± TET, ~100-fold less infectious virus was produced during vΔ*ind*I2 infections performed in the absence of TET compared to those performed in the presence of TET (Fig. 3C, left panel). These data indicate that repression of I2 has a significantly deleterious effect on the production of infectious viral progeny during a single round of infection on BSC40 cells. The same phenotype was observed in mouse L cells and human TK^- cells (not shown). The conclusion that I2L is an essential gene was further supported by our inability to generate a viral

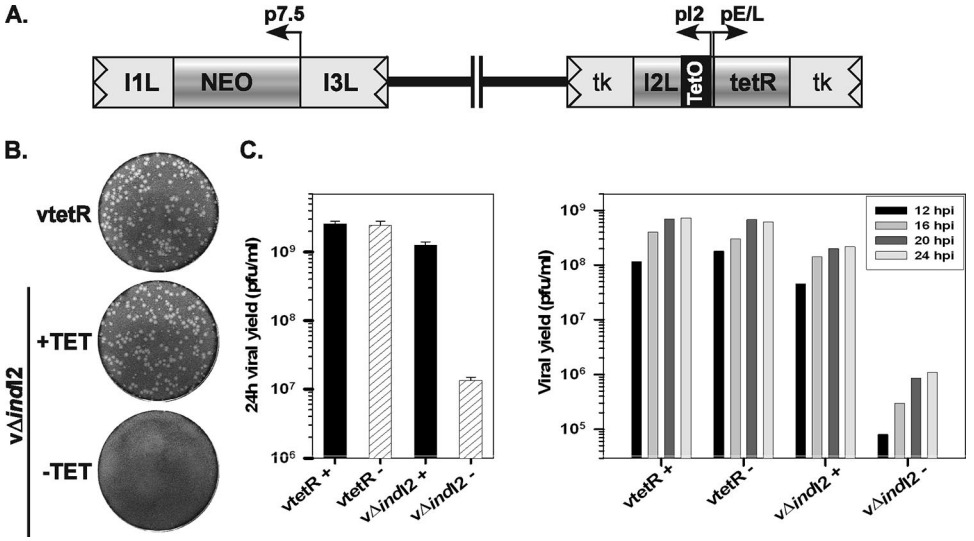

FIG. 3. Repression of I2 expression causes a dramatic reduction in the yield of infectious virus and blocks plaque formation. (A) Schematic representation of the relevant regions of the vΔ*ind*I2 genome. An inducible copy of the I2 gene, under the regulation of its own promoter and the Tet operator, as well the Tet repressor gene, was inserted into the nonessential TK locus. The endogenous I2 allele was replaced by NEO. HPI, hours postinfection. (B) Plaque assay. Confluent monolayers of BSC40 cells were infected with the parental virus vTetR or vΔ*ind*I2 in the presence (+) or absence (−) of TET for 48 h; plaques were visualized after crystal violet staining. (C) Quantitation of viral yield. Cells were infected with vTetR or vΔ*ind*I2 in the presence (+) or absence (−) of TET for 24 h (left graph) or for 12, 16, 20, and 24 h (right graph). The yield of total cell-associated virus was determined by titration on BSC40 cells in the presence of TET.

recombinant in which the endogenous I2L gene was deleted and replaced by a selectable marker (NEO) (data not shown).

Viral DNA replication, gene expression, and morphogenesis progress normally during nonpermissive vΔ*ind*I2 infections. Having determined that there was a severe decrease in the yield of infectious progeny when the expression of I2 was repressed, we wished to determine which stages of the viral life cycle were affected by the absence of I2. First, the temporal profile of viral gene expression was determined by metabolically labeling infected cells with [^{35}S]methionine at sequential times after infection and visualizing the profile of nascent protein synthesis by SDS-PAGE and autoradiography. The protein expression profiles were indistinguishable whether vΔ*ind*I2 infections were performed in the presence or absence of inducer (Fig. 4A).

The fact that late protein synthesis occurred with normal timing and intensity was an indication that viral DNA replication had also occurred, because DNA replication is a prerequisite for intermediate and late gene expression. Although it seemed unlikely that a membrane protein would play a role in the maturation of replication intermediates, we nevertheless examined whether the repression of I2 had any impact on the processing of concatemeric intermediates to monomeric genomes and found that it did not (data not shown).

Since the biochemical milestones in the viral life cycle seemed to be unaffected by the repression of I2, we next turned to the process of virion morphogenesis. First, we investigated whether the precursors of the major virion proteins underwent normal proteolytic processing in the absence of I2; these processing events occur only during the later stages of virion morphogenesis. We therefore performed pulse-chase analyses in cells infected with wt virus (Fig. 4B, lanes 1 to 6) or vΔ*ind*I2 virus (lanes 7 to 10) in the presence or absence of TET. Samples treated with RIF, an inhibitor of morphogenesis and hence of proteolytic processing (1, 34), were included as controls (lanes 5 and 6). The black arrows point to the precursors, whereas the gray arrows indicate the cleaved products. As expected, RIF inhibited processing during wt infections, whereas the inclusion or omission of TET had no effect on wt infections (compare lanes 2, 4, and 6). Most importantly, we observed that proteolytic processing was comparable when vΔ*ind*I2 virus infections were performed in the presence or absence of TET (compare lanes 8 and 10). These data indicate that the repression of I2 does not arrest virion assembly at an early stage.

To address the question of virion morphogenesis in more detail, we performed ultrastructural analysis of cells infected with vΔ*ind*I2 for 18 h in the presence or absence of inducer. In both cases, the full set of assembly intermediates, including electron-dense virosomes, membrane crescents, immature virions (IV), immature virions with nucleoid (IVN), and mature virions (MV) were observed. (Representative images for vΔ*ind*I2 without TET infections are shown in Fig. 4C.) Morphogenesis was clearly able to proceed to completion in the absence of I2. Although a formal quantitation of intermediates versus MV was not performed, there appeared to be a modest increase in the number of IV and IVN forms and a modest decrease in the number of MV when I2 was repressed. These data suggested that morphogenesis might proceed at a somewhat slower rate when I2 is repressed. However, when cells were infected with and without TET and the viral yields were titrated at 12, 16, 20, and 24 hpi (MOI of 3 [Fig. 3C, right graph]), we observed that viral yield appeared to plateau at 20 hpi in all cases. Thus, repression of I2 appears to block, rather than delay, the production of infectious virus.

During vaccinia virus infections, a subset of virions become

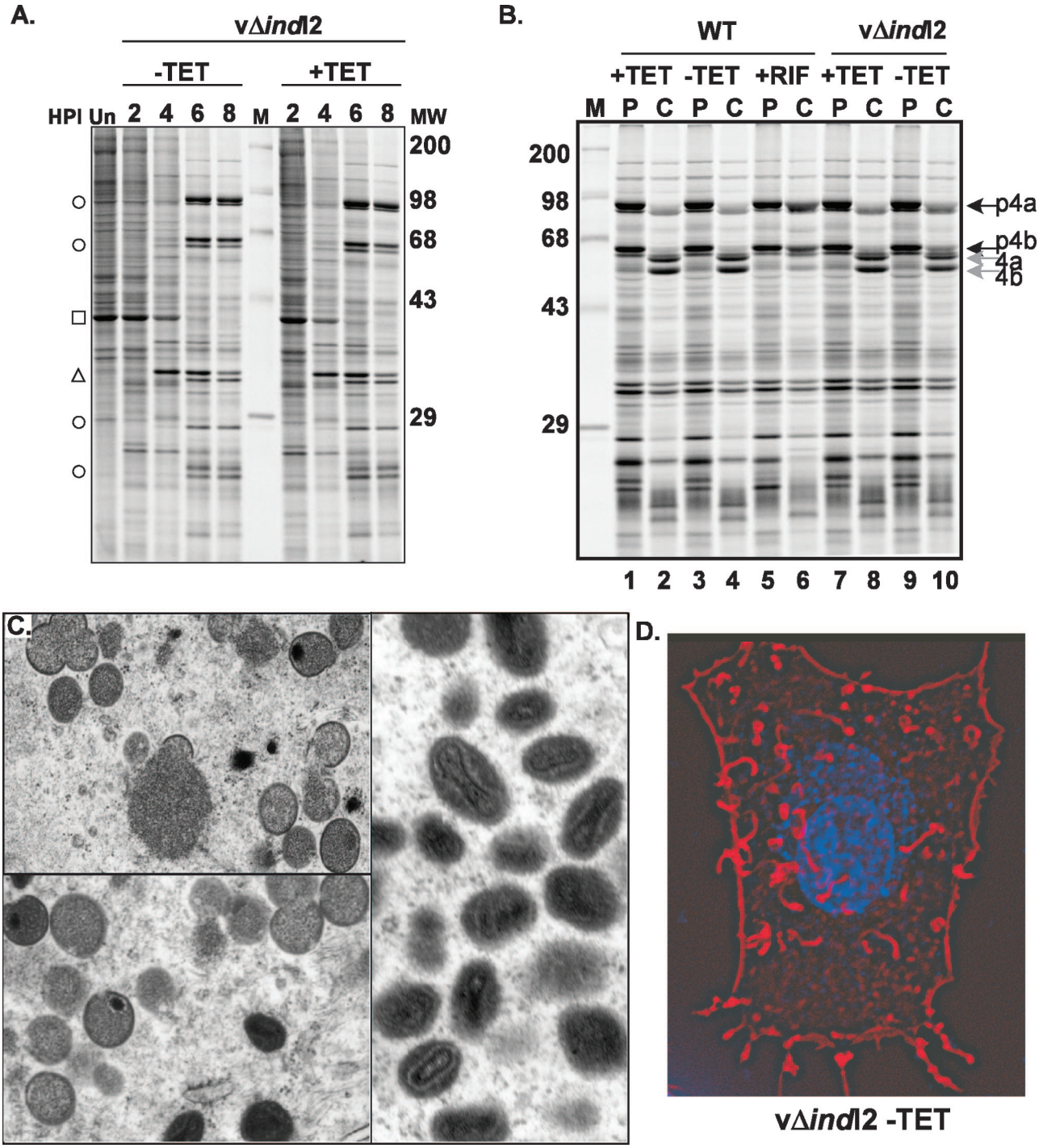

FIG. 4. I2 repression does not block viral gene expression or morphogenesis. (A) Temporal profile of viral protein synthesis. BSC40 cells were infected vΔ*ind*I2 (±TET) and pulse-labeled with [^{35}S]methionine at sequential times after infection as indicated (2, 4, 6, and 8 hpi). Lysates were resolved by SDS-PAGE and visualized by autoradiography. The molecular masses of ^{14}C protein standards (M) are indicated to the right (in kDa). Representative intermediate proteins are indicated by triangles and late proteins by circles; the cellular protein actin is indicated by a square. (B) Proteolytic processing of core proteins. BSC40 cells were infected with wt virus (lanes 1 to 6) or vΔ*ind*I2 (lanes 7 to 10) in the presence (+) or absence (−) of TET. RIF was included where indicated (lanes 5 and 6). At 8 hpi, cells were pulse-labeled with [^{35}S]Met for 45 min before being harvested immediately (pulse [P]) or refed with complete media and incubated for an additional 15 h (chase [C]). Cell lysates were resolved by SDS-PAGE and visualized by autoradiography. ^{14}C protein standards are shown to the left (M), with their molecular masses indicated (in kDa). The precursor forms of the core proteins 4a and 4b are indicated by black arrows, while the processed mature forms are indicated by gray arrows. (C) Electron microscopic analysis of vΔ*ind*I2 infections. BSC40 cells were infected with vΔ*ind*I2 in the presence (not shown) or absence of TET for 18 hpi and examined by transmission electron microscopy. Mature virions and the full range of morphogenesis intermediates were observed in both samples. (D) Visualization of actin tails. BSC40 cells were infected with vΔ*ind*I2 (MOI of 2) in the absence (or presence [not shown]) of TET; at 18 hpi, cells were fixed and stained with Texas Red-phalloidin to visualize actin tails (and DAPI to visualize cellular and viral DNA).

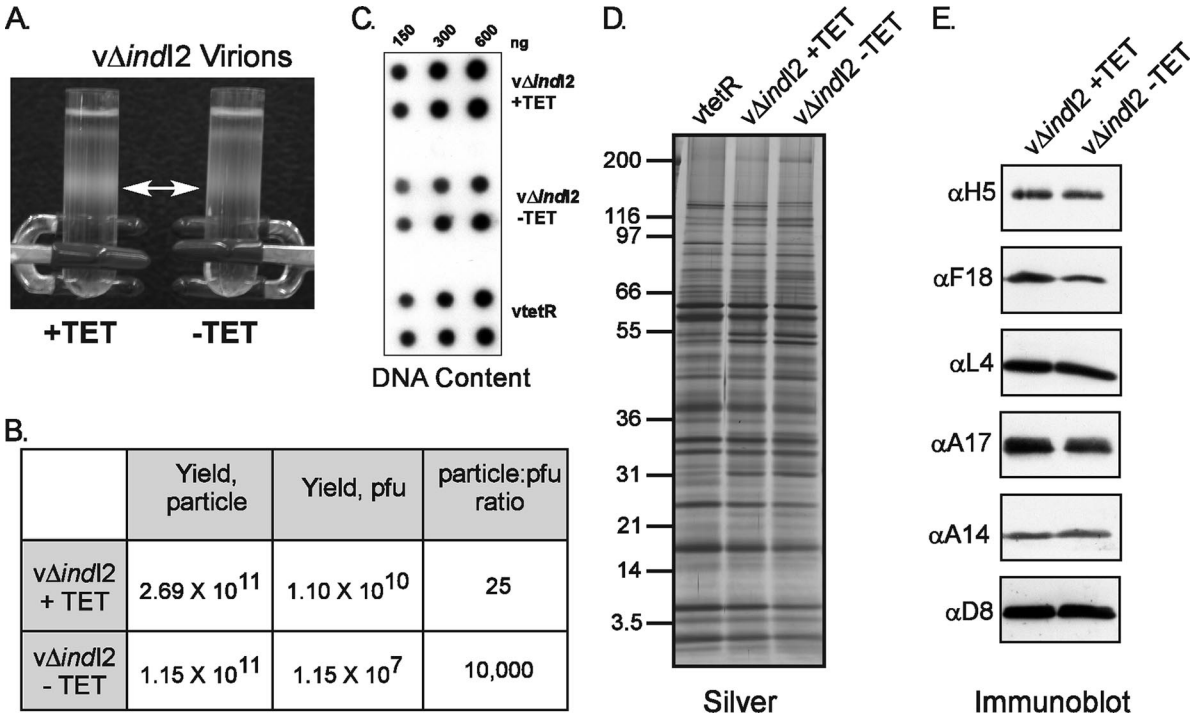

B.

	Yield, particle	Yield, pfu	particle:pfu ratio
vΔ*ind*I2 + TET	2.69×10^{11}	1.10×10^{10}	25
vΔ*ind*I2 - TET	1.15×10^{11}	1.15×10^{7}	10,000

FIG. 5. I2-deficient virions have a normal protein and DNA complement but are greatly reduced in specific infectivity. (A) Virion purification. BSC40 cells were infected with vTetR (not shown) or vΔ*ind*I2 (±TET) (MOI of 5), and virions were purified by sedimentation through a 36% sucrose cushion and a 25 to 40% sucrose gradient. The light-scattering bands of virions are indicated by the white arrow. (B) Quantitation of particle yield and infectious yield. The yields of virion particles and infectious virus were quantitated by measuring the OD_{260} and by plaque assay titration, respectively. (C) Determination of DNA content. One hundred fifty, 300, and 600 ng of purified vTetR, $I2^+$ and $I2^-$ virions were subjected to Southern dot blot hybridization using a probe representing fragments of the vaccinia virus genome. (D and E) Equal amounts of vTetR, I2+, and $I2^-$ virions were resolved by SDS-PAGE and subjected to silver staining (D) or immunoblot (E) analysis with antisera specific for the H5, F18, L4, A17, A14, and D8 proteins (αH5 to αD8, respectively).

enwrapped in double membranes derived from the Golgi apparatus, traffic to the cell surface on microtubules, and are released by exocytosis (50). Many of these extracellular virions (EV) remain tethered to the cell surface and initiate actin tail formation, which propels the EV toward adjacent cells and facilitates viral spread (49, 50). In our ultrastructural analyses, we observed numerous wrapped MV, also known as intracellular enveloped virions. To confirm that the process of EV formation was not impaired by the absence of I2, we assayed for the formation of actin tails in vΔ*ind*I2 infections performed in the absence of inducer. Infected cells were stained with Texas Red-conjugated phalloidin and examined by immunofluorescence microscopy; actin tails were easily observed in cells infected with vΔ*ind*I2 in the absence of inducer (Fig. 4D). As a control, we confirmed that these actin tails were absent when infections were performed in the presence of brefeldin A (not shown), which blocks the formation of EV (58).

Analysis of the protein and DNA profile of I2-containing and I2-deficient virions. Since the assembly of mature virions did not appear to be compromised in the absence of I2, we purified I2-containing and I2-deficient virions and examined their protein and DNA content. As shown in Fig. 5A, I2-containing and I2-deficient virions form a light-scattering band at the same position. The particle yield from vΔ*ind*I2 infections performed in the absence of TET was decreased by ~2.3-fold compared to the yield from induced infections, but the yield of infectious virus was reduced by ~1,000-fold (Fig. 5B). This 400-fold increase in the particle/PFU ratio of the I2-deficient virions indicates that they have an extremely low specific infectivity.

The DNA content of the purified virions was measured by dot blot hybridization (Fig. 5C), the overall protein content was assessed by silver stain analysis (Fig. 5D), and the presence of specific virion proteins was examined by immunoblot analysis (Fig 5E). No significant difference was observed between the I2-containing and I2-deficient virions in any of these assays.

$I2^-$ virions do not induce CPE and do not direct early gene expression. Although the I2-deficient virions appeared to encapsidate the normal profile of proteins and DNA, they were not infectious. We therefore wanted to address at which stage this poor infectivity was first manifested and began by assessing their ability to direct early gene expression or induce cytopathic effect (CPE). Cells were infected with equivalent numbers of $I2^+$ and $I2^-$ virions (corresponding to an MOI of 10 for the $I2^+$ virions) and then maintained in the presence of [^{35}S]methionine. The morphology of the cells was assessed at 4 hpi, and it was evident that the $I2^-$ virions did not induce the morphological changes, such as cell rounding, that were so obvious in cells infected with the $I2^+$ virions (Fig. 6A). Early gene expression was then assessed by harvesting the cells at 4 hpi and performing immunoprecipitation analyses with antibodies directed against a variety of early viral proteins (anti-

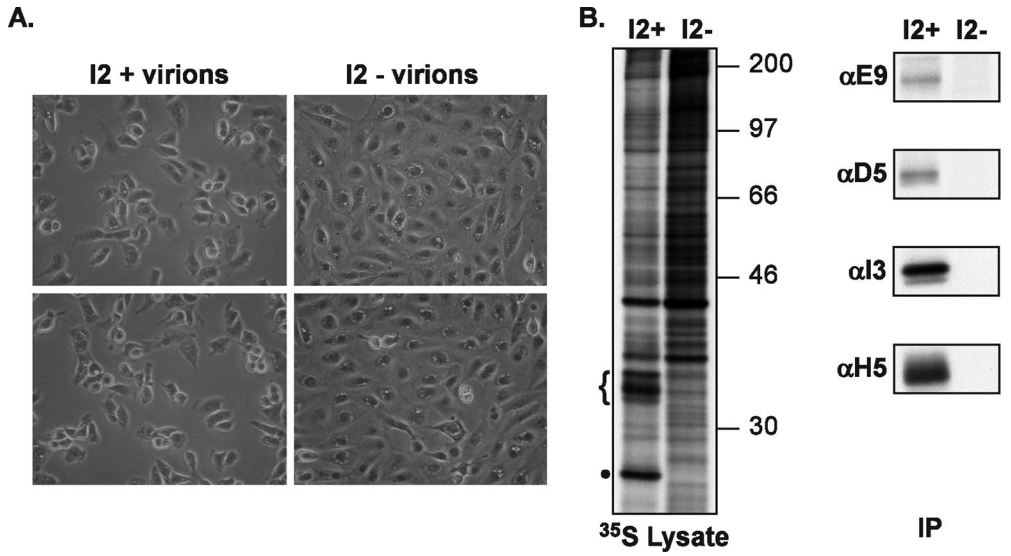

FIG. 6. I2-deficient virions do not induce CPE or mediate early gene expression in target cells. (A) Visualization of CPE. BSC40 cells were infected with $I2^+$ (left panels) or $I2^-$ (right panels) virions (MOI of 10) in the presence of [^{35}S]Met. At 4 hpi, the cells were visualized by phase-contrast microscopy; representative images are shown. (B) Analysis of early gene expression. Lysates prepared from the infections described in panel A were either resolved electrophoretically and examined by autoradiography (left panel) or subjected to immunoprecipitation (IP) analysis with antibodies directed against the early viral proteins E9, D5, I3, and H5 (αE9 to αH5, respectively [right panel]) and then visualized by autoradiography. The brace symbol and dot indicate early viral proteins that are evident in the cells infected with $I2^+$, but not $I2^-$, virions. The molecular masses of ^{14}C protein standards (in kDa) are indicated to the right of the autoradiograph.

E9, -D5, -I3, and -H5) (12, 15, 25, 30, 38, 42). Autoradiographs of the lysates and immunoprecipitates are shown in Fig. 6B. In cells infected with the I2-deficient virions, the synthesis of host proteins persisted and no expression of early viral proteins was detected, in stark contrast to the pattern observed after infection with $I2^+$ virions. Thus, infection with I2-deficient virions was shown to arrest prior to the synthesis of early proteins.

Virion entry is dependent on the presence of I2 in the virion. The stages of infection that precede early protein synthesis include binding to target cells, entry into target cells, and transcription of early genes. Because I2 is a membrane protein, we deemed it far more likely that its absence would affect binding or entry rather than transcription. To test this prediction directly, we used the immunofluorescence-based assay that has been established to monitor virion binding and entry (48, 61). Cells were inoculated with 300 particles/cell of $I2^+$ or $I2^-$ virions at 4°C for 1 h and then either processed for immunofluorescence microscopy or shifted to 37°C for 1.5 h in the presence of cycloheximide. Virions bound to the cell surface were identified with an antibody to the A17 membrane protein (32, 56), and virion cores deposited in the cytoplasm after virion entry were detected with an antibody to the A5 core protein (10). As shown in Fig. 7, the anti-A17 antibody readily detected virions bound to cells after adsorption of either $I2^+$ or $I2^-$ virions at 4°C; these virions appear as brightly stained green puncta on the cell surface. These data indicate that I2 is not required for virus attachment. As expected, no staining was observed with the anti-A5 serum under these conditions, as the A5 epitope is not available in intact virions. In the cells that had been infected with $I2^+$ virions and then shifted to 37°C, numerous A5-positive green puncta were observed, indicative of the unmasking of the A5 antigen upon deposition of the viral cores within the cytoplasm. However, no such staining was observed in cells that had been infected with the $I2^-$ virions, strongly suggesting that virion entry depends upon the presence of the I2 protein.

$I2^-$ virions do not induce acid-induced cell-cell fusion. Another assay that serves as a surrogate measure of virion entry is the "fusion-from-without" assay, which evaluates the ability of viral inocula to mediate cell fusion at acid pH (19, 48). The validity of this assay has been strengthened by recent demonstrations that proteins required for virion entry are also required for cell fusion, such as A28 and H2 (46, 48). Cultures were therefore inoculated with a high dose of vTetR (parental virus) or $I2^+$ or $I2^-$ virions at 4°C for 1 h. The cells were then either left in neutral medium (pH 7.4) or briefly exposed to acidic medium (pH 5.5) and then incubated at 37°C for 3 h in the presence of cycloheximide. Cell fusion was monitored by phase-contrast microscopy; representative images are presented in Fig. 8 (right panel). None of the infections maintained at neutral pH showed any evidence of cell fusion (left panels). However, multinucleate syncytia were evident in cells that had been infected with vTetR or $I2^+$ virions and subjected to the pH 5 pulse (Fig. 8, right panels, arrows indicate large syncytium). In contrast, $I2^-$ virions were unable to trigger syncytium formation after acid treatment. These data provide further support for the conclusion that the I2 protein is essential for virion entry. In data not shown here, we also performed the "fusion-from-within" assay, in which CEV deposited on the cell surface during infection are assayed for their ability to trigger cell fusion after an acidic pulse (19, 48). Here again, $I2^+$ but not $I2^-$ virions triggered cell fusion (data not shown).

I2-deficient virions contain reduced levels of some of the proteins previously identified as essential for virion entry. During the course of these studies, numerous other proteins have been shown to play essential roles in vaccinia virus entry,

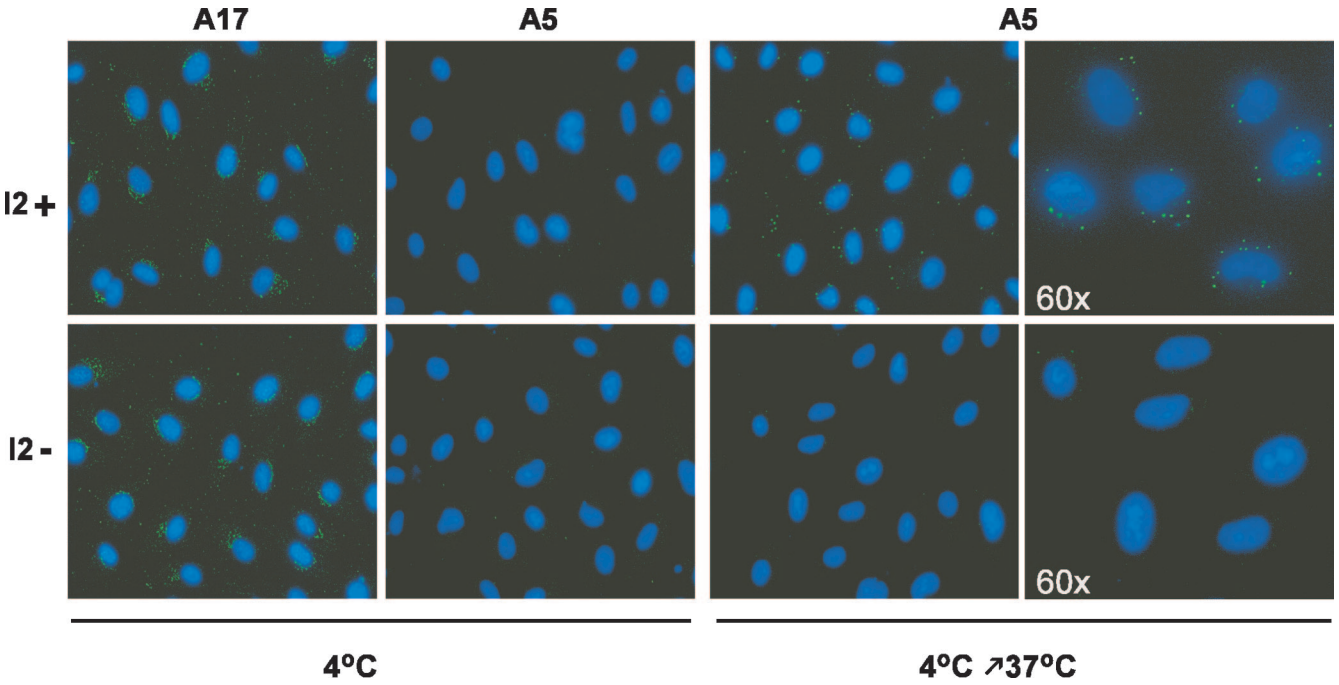

FIG. 7. I2-deficient virions can bind to target cells but are deficient in entry. BSC40 cells were infected with 300 particles of $I2^+$ or $I2^-$ virions (in duplicate) and maintained on ice for 1 h. One set of samples was fixed immediately (4°C), whereas a second set was incubated for at 37°C for 2 h in complete medium containing 300 μg/ml cycloheximide before being fixed (from 4°C to 37°C). Cells were permeabilized and stained with anti-A17 (left panels) or anti-A5 (right panels) sera. DAPI was added to visualize nuclei.

and many of these interact to form a multiprotein entry/fusion complex (EFC) (3, 36, 37, 46–48, 52, 53, 57). We therefore addressed the question of whether repression of I2 might compromise the encapsidation of other proteins involved in virion entry. As shown in Fig. 9, I2-deficient virions contained reduced levels of the A21, G3, and A28 proteins; the levels of these proteins were reduced fivefold from what was observed in $I2^+$ virions. This result stands in contrast to the encapsidation of normal levels of other components of the virion membrane (A13, A17, and A14) or core (L4, F10, and A5).

Identification of amino acid motifs required for I2 function. As shown in Fig. 1, I2 is a small protein with a hydrophilic N-terminal tail and a C-terminal hydrophobic domain that we assume serves as a membrane-anchoring domain. To gain an initial understanding of which domains and/or residues within the protein might be important for I2's biological function, we established a transient complementation assay. In this assay, cells were infected with vΔ*ind*I2 in the absence of TET and transfected with an empty vector or one containing various alleles of I2 under the regulation of a strong late promoter. We examined the wt I2 allele, an allele lacking the C-terminal membrane-anchoring domain (not shown), an allele lacking the N-terminal 12 aa, or alleles containing alanine substitution mutations at positions of clustered charged or aromatic residues. A graphic representation of these data is shown in Fig. 10, along with an immunoblot analysis documenting the expression of the various transfected alleles. When TET was omitted from the medium, there was a 3-log difference in the viral yield that was not affected by transfection of an empty vector. The plasmid encoding wt I2 restored virus yield to the level seen when inducer was present; as shown in the immunoblot, the protein expressed from the transfected plasmid is present at levels that significantly exceed that of the endogenous protein, which is undetectable in this experiment. The allele encoding an I2 derivative lacking the C-terminal membrane-spanning domain lacked complementation activity, but we were also unable to detect the protein (not shown). We interpreted these data as evidence that, without the membrane-anchoring domain, the protein was highly unstable. Deletion of the highly conserved N-terminal 12 aa (Δ1–12) also resulted in a complete loss of complementation activity, although this protein was expressed as well as the wt protein. (Note that this protein has an anomalous electrophoretic migration, since it lacks 12 aa but comigrates with the wt protein.) Mutation of any of three clusters of charged residues, $E^{17}DD\rightarrow AAA$, $D^{2}K\rightarrow AA$, and $D^{33}EK\rightarrow AAA$, had no effect on complementation activity. All of these mutants except $E^{17}DD$ were readily detected by the anti-I2 serum. Mutation of the $E^{17}DD$ motif may disrupt the epitope recognized by the serum, as there is complete restoration of virus production in the presence of the mutation but no reactivity in the immunoblot. We next mutated two conserved hydrophobic regions. One allele, in which Y^{5}, F^{9}, and F^{12} were mutated to alanine, retained wt complementation activity. More importantly, the second allele, which contained $F^{23}I\rightarrow AA$ substitutions, was unable to complement the I2 deficiency despite being expressed at high levels.

DISCUSSION

The heretofore unstudied protein I2 is encoded by one of the 90 genes that is conserved in all chordopoxviruses. I2L is

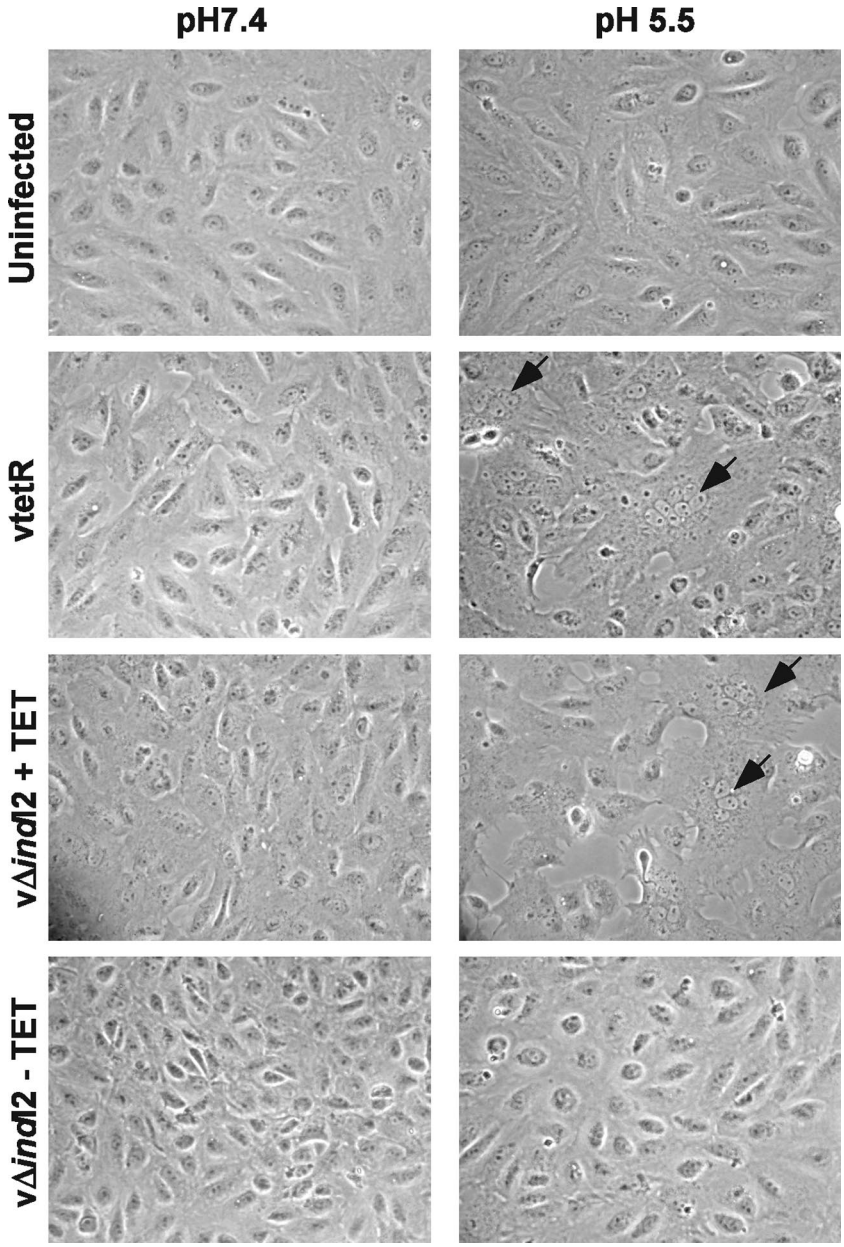

FIG. 8. I2-deficient virions cannot mediate fusion from without. BSC40 cells were incubated with 10,000 particles per cell of purified vTetR, $I2^+$, or $I2^-$ virions. After 1 h of absorption at 4°C, the cells were washed and subjected to a brief pulse with pH 5.5 or pH 7.4 medium. Cells were washed and incubated at 37°C for 3 h in the presence of cycloheximide. Phase-contrast microscopy images are presented. The arrows indicate syncytia formed by virion-mediated acid-induced fusion (right panels).

predicted to encode a protein of 73 aa, and we have verified that the protein is indeed expressed at late times of infection. Using a recombinant virus encoding HA-tagged I2 from the endogenous locus, we also showed that the I2 protein is packaged in mature virions; fractionation studies indicate that I2 is found in the membrane of purified virions. Given our results, it is somewhat surprising that I2 was not identified as a virion component in recent studies profiling the composition of virions by mass spectroscopy (6, 41, 65). We attributed this discrepancy to the fact that I2 is a very small protein and may also be present at low copy number. The I2 protein can be extracted from the virion membrane with NP-40 alone, as can the A13 protein, which is also a very small protein that contains a single membrane-spanning domain (32, 59). In contrast, the A14 and A17 proteins, which form inter- and intramolecular disulfide bonds and each span the membrane twice, can only be extracted with NP-40 and DTT (32). The integral association of I2 with membranes in vivo and the incorporation of I2 into the virion membrane are likely to be mediated by the extremely hydrophobic domain present at the C terminus of the protein. Because this domain is required for stable expression of the protein, we could not directly test the hypothesis that it serves as a membrane targeting domain for I2.

To address the function of I2 in the viral life cycle, we

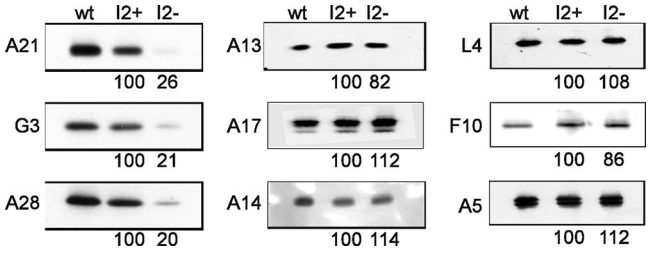

FIG. 9. I2-deficient virions contain reduced levels of some components of the EFC. Three micrograms of purified wt, $I2^+$, or $I2^-$ virions were resolved by SDS-PAGE and subjected to immunoblot analysis with antisera specific for components of the EFC (A21, G3, and A28), membrane proteins involved in virion morphogenesis (A13, A14, and A17), or core components (L4, F10, and A5). For each blot, the level of protein present in the $I2^+$ virions was set at 100, and the relative level present in the $I2^-$ virions was determined.

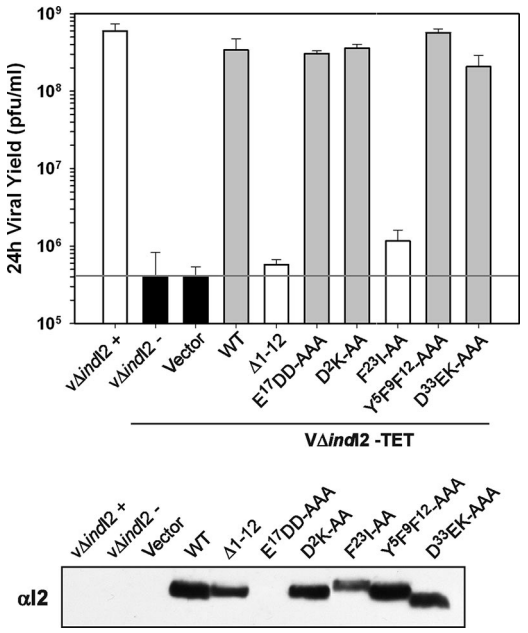

FIG. 10. The biological activities of various I2 alleles can be monitored via transient complemention of vΔ*ind*I2. BSC40 cells were infected with vΔ*ind*I2 ($\pm$TET); at 3 hpi, cells were transfected with empty vector or plasmids encoding wt or mutant alleles of I2 under the regulation of a viral promoter. Cells were harvested at 24 hpi, and plaque assays were performed to determine the viral yield. The data are shown graphically in the top panel, with the horizontal line representing the baseline yield obtained from uninduced infections. A portion of the harvested cells was also resolved by SDS-PAGE, and the expression of the plasmid-borne I2 protein was verified by immunoblot analysis with anti-I2 antibody (αI2). The I2 protein expressed from the viral genome is below the level of detection in this experiment.

generated an inducible recombinant in which the expression of I2 from its own promoter was dependent upon inclusion of TET in the culture medium. When I2 was repressed, gene expression, DNA replication, and genome maturation proceeded normally. Moreover, core proteins appeared to undergo normal proteolytic processing, and electron microscopic analysis confirmed that the full spectrum of morphogenetic intermediates was present. Mature virions were readily detected, as were wrapped and enveloped viruses. However, the yield of infectious virus at 24 hpi was reduced by 100- to 1,000-fold in the absence of I2. Virion production was not compromised, but the particle/PFU ratio of the I2-deficient virions was ~400 fold greater than that of those containing I2. Nevertheless, these I2-deficient virions had a wt appearance and contained a normal complement of protein and genomic DNA.

The infectivity defect seen with the I2-deficient virions manifested itself at an early stage. These virions did not induce any CPE, nor were they able to direct the synthesis of early proteins. Furthermore, they were also unable to mediate "fusion from without": cells inoculated with $I2^-$ virions did not induce syncytia after being pulsed with pH 5.5. Acid-induced syncytium formation is now known to mimic viral entry: the brief treatment with low pH mimics the environment presented by the endosomal pathway of entry/fusion that can be utilized efficiently by poxvirus particles (51, 54). This suggestion that I2-deficient virions were defective in virion entry was reinforced by immunofluorescence analysis, which verified that I2-deficient virions retain the ability to bind to target cells but lack the ability to enter cells, as defined by deposition of subviral cores within the cytoplasm.

Binding to target cells is mediated, at least in part, by the association of several virion proteins (A27, H3, and D8) with GAGs on the cell surface as well as the interaction of the A26 protein with laminin (5, 7, 22, 23, 29). There is a presumption that a higher-affinity and/or more specific interaction must take place between as-yet-unknown virion proteins and cellular receptor(s). Neutralizing antibodies have been generated to the H3, A27, and L1 proteins. H3 and A27 are not essential for the production of infectious virus, making them unlikely candidates for receptor-binding proteins. The possibility that L1 may play this role has been difficult to test, because repression of L1 has been shown to block the assembly of mature virions (40). Thus, we cannot be sure how virions that are positive for GAG and laminin interactions, but negative for receptor interactions, would score in the virion binding assay. We are therefore following convention in saying that I2-deficient virions can bind to cells, but we cannot rule out that the possibility that I2 may indeed contribute, either directly or indirectly, to the establishment of a "binding state" that may be a prerequisite for entry.

Production of viral particles that bind to, but cannot enter, cells has recently been associated with mutations in numerous vaccinia virus genes. The A16, A21, A28, G3, G9, H2, J5, L5, and F9 proteins have been shown to be dispensable for virion morphogenesis and cell attachment but essential for core deposition into the host cell (3, 24, 36, 37, 46–48, 52, 53, 57). A conserved feature shared by all but one of these proteins (G3) is the presence of disulfide bonds formed by the virally encoded redox machinery. Eight of these proteins (all but F9) have been shown to associate in a multiprotein complex now known as the EFC (47). The role of individual proteins within the complex is just beginning to be deciphered, but it is known that the EFC does not form in the absence of the virion membrane, nor does it form if either A21 or A28 are absent. H2 and A28 are known to interact directly (35). The F9 protein associates with the EFC at substoichiometric levels but is not required for EFC formation (3). F9 shows significant sequence

similarity to the L1 protein, which was previously found to play a role in virion morphogenesis (40). However, very recent data show instead that L1 is dispensable for virion morphogenesis but, like F9, associates with the EFC and is essential for virion entry (2).

The EFC has also been shown to associate with a heterodimeric complex containing the A56 (HA) and K2 proteins, which are known as fusion regulatory proteins. This interaction is mediated by A16 and G9 (62, 63). In the absence of either A56 or K2, infected cells form syncytia spontaneously at neutral pH. These data led to the hypothesis that the A56/K2 proteins prevent syncytium formation by interacting with A16/G9 and blocking EFC-mediated fusion. It seems reasonable to propose that, during the entry of wt viruses, the EFC-A56/K2 interaction is disrupted in the acidic environment of the endosome, activating fusion of the virion and vesicular membranes and resulting in core release.

The data presented here indicate that the I2 protein is the 10th protein that is required for virion entry. Although I2 was not identified as part of the EFC, its presence within the EFC is still possible. It may have been overlooked because of its small size (molecular weight of 8,000), or it may, like the F9 and L1 proteins, be present in substoichiometric levels (3). A fivefold reduction in the levels of some of the EFC proteins was observed within I2-deficient virions, suggesting that I2 might play a role in the stabilization of the EFC or in recruitment of EFC proteins to nascent virion membranes. This 5-fold reduction in EFC proteins seems unlikely to account for the 400-fold decrease in the specific infectivity of the I2-deficient virions. However, it may be that the fivefold reduction does indeed bring the level of the EFC below a threshold needed for efficient entry; it is also possible that the reduction in EFC proteins is greater than our immunoblot analyses indicate. Alternatively, I2 might contribute to virion entry in an EFC-independent manner.

The small size of the I2 protein and the absence of disulfide bonds make I2 quite distinct from the entry proteins that comprise the EFC. One of the striking features that emerges from comparative analysis of the I2 orthologs present in diverse poxviruses is the C-terminal hydrophobic domain. We propose that this region is a membrane targeting domain (MTD) that, like the MTDs of the poxviral H3 protein (11) and other tail-anchored proteins, mediates posttranslational insertion of I2 into nascent virions, although cotranslational insertion is also possible. The N-terminal portion of the protein contains several highly conserved regions. Results from a limited structure/function analysis revealed that three clusters of charged residues within this portion are not essential for I2's biological function. However, the highly conserved N-terminal 12 aa, which are also hydrophobic in character, are required. Similarly, perturbation of a small hydrophobic/aromatic cluster ($FI^{23}I^{24}$) within this N-terminal domain renders I2 biologically inactive. The hydrophobic and aromatic residues within the N-terminal domain of I2 may mediate protein-protein interactions within the virion membrane or between the virion and the target cell. Alternatively, the N terminus of I2 may participate directly in membrane fusion.

The process through which poxviruses enter cells has recently become an area of intense study. First, it seems striking that at least 11 viral proteins are required for entry. Second, new insights into the mechanism of entry itself are emerging rapidly. Historically, fusion of the virion membrane with the plasma membrane was thought to occur (4, 13, 33). More recently, it has emerged that the majority of virions are internalized into an endosomal compartment, with subsequent membrane fusion and cytoplasmic core deposition occurring only upon compartment acidification (51, 54). The initial internalization of virions has recently been shown to occur via macropinocytosis, a process which is upregulated when the binding of virions to cells induces PAK1-mediated signaling events that result in massive cell blebbing (31). Macropinocytic uptake requires the presence of phosphatidylserine in the virion membrane, suggesting that virion uptake mimics the engulfment of apoptotic fragments. The presence of cholesterol in the plasma membrane of the target cell has also been shown to be important for virion entry (8).

Deposition of the subviral core within the cytoplasm requires fusion of the virion membrane with the membrane of an endocytic compartment (or, less frequently, with the plasma membrane). Because none of the EFC proteins has been shown to have fusogenic activity, we have no insight into how this process occurs. The viral A17 protein has been shown to mediate cell-cell fusion when expressed at high levels on its own in insect cells and to do so when coexpressed with the A27 protein in mammalian cells (26). Because A17 is essential for the early stages of virion morphogenesis (28, 43, 44, 64), it has not been possible to test its role in virion entry. Thus, a role for A17 as a mediator of fusion in the context of infection remains to be formally tested.

The intricacy of the poxvirus life cycle has proven to be illuminating for virologists, immunologists, and cell biologists alike. Recent studies have shown that process of poxvirus entry is surprisingly complex, and further study of how I2 collaborates with many other viral proteins to facilitate the initial interactions of poxvirus virions with their target cells should prove to be of great interest.

ACKNOWLEDGMENTS

This work was sponsored by the NIH/NIAID Regional Center of Excellence for Bio-Defense and Emerging Infectious Diseases Research (RCE) Program. We acknowledge membership within and support from the Region V "Great Lakes" RCE (NIH award 1-U54-AI-057153). P.T. also acknowledges the support of NIH RO1 063630.

We thank Angelika for technical support and Clive Wells for excellent assistance with electron microscopy and acknowledge the invaluable input of all of the members of the Traktman laboratory.

REFERENCES

1. **Bayliss, C. D., and R. C. Condit.** 1995. The vaccinia virus A18R gene product is a DNA-dependent ATPase. J. Biol. Chem. **270:**1550–1556.
2. **Bisht, H., A. S. Weisberg, and B. Moss.** 2008. Vaccinia virus L1 protein is required for cell entry and membrane fusion. J. Virol. [Epub ahead of print.] doi:10.1128/JVI.00852-08.
3. **Brown, E., T. G. Senkevich, and B. Moss.** 2006. Vaccinia virus F9 virion membrane protein is required for entry but not virus assembly, in contrast to the related L1 protein. J. Virol. **80:**9455–9464.
4. **Carter, G. C., M. Law, M. Hollinshead, and G. L. Smith.** 2005. Entry of the vaccinia virus intracellular mature virion and its interactions with glycosaminoglycans. J. Gen. Virol. **86:**1279–1290.
5. **Chiu, W.-L., C.-L. Lin, M.-H. Yang, D.-L. M. Tzou, and W. Chang.** 2007. Vaccinia virus 4c (A26L) protein on intracellular mature virus binds to the extracellular cellular matrix laminin. J. Virol. **81:**2149–2157.
6. **Chung, C.-S., C.-H. Chen, M.-Y. Ho, C.-Y. Huang, C.-L. Liao, and W. Chang.** 2006. Vaccinia virus proteome: identification of proteins in vaccinia virus intracellular mature virion particles. J. Virol. **80:**2127–2140.
7. **Chung, C.-S., J.-C. Hsiao, Y.-S. Chang, and W. Chang.** 1998. A27L protein

mediates vaccinia virus interaction with cell surface heparan sulfate. J. Virol. **72:**1577–1585.
8. **Chung, C.-S., C.-Y. Huang, and W. Chang.** 2005. Vaccinia virus penetration requires cholesterol and results in specific viral envelope proteins associated with lipid rafts. J. Virol. **79:**1623–1634.
9. **Condit, R. C., N. Moussatche, and P. Traktman.** 2006. In a nutshell: structure and assembly of the vaccinia virion. Adv. Virus Res. **66:**31–124.
10. **Cudmore, S., R. Blasco, R. Vincentelli, M. Esteban, B. Sodeik, G. Griffiths, and J. Krijnse Locker.** 1996. A vaccinia virus core protein, p39, is membrane associated. J. Virol. **70:**6909–6921.
11. **da Fonseca, F. G., E. J. Wolffe, A. Weisberg, and B. Moss.** 2000. Characterization of the vaccinia virus H3L envelope protein: topology and posttranslational membrane insertion via the C-terminal hydrophobic tail. J. Virol. **74:**7508–7517.
12. **DeMasi, J., and P. Traktman.** 2000. Clustered charge-to-alanine mutagenesis of the vaccinia virus H5 gene: isolation of a dominant, temperature-sensitive mutant with a profound defect in morphogenesis. J. Virol. **74:**2393–2405.
13. **Doms, R. W., R. Blumenthal, and B. Moss.** 1990. Fusion of intra- and extracellular forms of vaccinia virus with the cell membrane. J. Virol. **64:**4884–4892.
14. **Elroy-Stein, O., T. R. Fuerst, and B. Moss.** 1989. Cap-independent translation of mRNA conferred by encephalomyocarditis virus 5′ sequence improves the performance of the vaccinia virus/bacteriophage T7 hybrid expression system. Proc. Natl. Acad. Sci. USA **86:**6126–6130.
15. **Evans, E., and P. Traktman.** 1987. Molecular genetic analysis of a vaccinia virus gene with an essential role in DNA replication. J. Virol. **61:**3152–3162.
16. **Franke, C. A., C. M. Rice, J. H. Strauss, and D. E. Hruby.** 1985. Neomycin resistance as a dominant selectable marker for selection and isolation of vaccinia virus recombinants. Mol. Cell. Biol. **5:**1918–1924.
17. **Fuerst, T. R., E. G. Niles, F. W. Studier, and B. Moss.** 1986. Eukaryotic transient-expression system based on recombinant vaccinia virus that synthesizes bacteriophage T7 RNA polymerase. Proc. Natl. Acad. Sci. USA **83:**8122–8126.
18. **Fujiki, Y., A. L. Hubbard, S. Fowler, and P. B. Lazarow.** 1982. Isolation of intracellular membranes by means of sodium carbonate treatment: application to endoplasmic reticulum. J. Cell Biol. **93:**97–102.
19. **Gong, S. C., C. F. Lai, and M. Esteban.** 1990. Vaccinia virus induces cell fusion at acid pH and this activity is mediated by the N-terminus of the 14-kDa virus envelope protein. Virology **178:**81–91.
20. **Grubisha, O., and P. Traktman.** 2003. Genetic analysis of the vaccinia virus I6 telomere-binding protein uncovers a key role in genome encapsidation. J. Virol. **77:**10929–10942.
21. **Ho, Y., J. C. Hsiao, M. H. Yang, C. S. Chung, Y. C. Peng, T. H. Lin, W. Chang, and D. L. Tzou.** 2005. The oligomeric structure of vaccinia viral envelope protein A27L is essential for binding to heparin and heparan sulfates on cell surfaces: a structural and functional approach using site-specific mutagenesis. J. Mol. Biol. **349:**1060–1071.
22. **Hsiao, J.-C., C.-S. Chung, and W. Chang.** 1998. Cell surface proteoglycans are necessary for A27L protein-mediated cell fusion: identification of the N-terminal region of A27L protein as the glycosaminoglycan-binding domain. J. Virol. **72:**8374–8379.
23. **Hsiao, J.-C., C.-S. Chung, and W. Chang.** 1999. Vaccinia virus envelope D8L protein binds to cell surface chondroitin sulfate and mediates the adsorption of intracellular mature virions to cells. J. Virol. **73:**8750–8761.
24. **Izmailyan, R. A., C.-Y. Huang, S. Mohammad, S. N. Isaacs, and W. Chang.** 2006. The envelope G3L protein is essential for entry of vaccinia virus into host cells. J. Virol. **80:**8402–8410.
25. **Klemperer, N., W. McDonald, K. Boyle, B. Unger, and P. Traktman.** 2001. The A20R protein is a stoichiometric component of the processive form of vaccinia virus DNA polymerase. J. Virol. **75:**12298–12307.
26. **Kochan, G., D. Escors, J. M. Gonzalez, J. M. Casasnovas, and M. Esteban.** 2008. Membrane cell fusion activity of the vaccinia virus A17-A27 protein complex. Cell. Microbiol. **10:**149–164.
27. **Koerner, T. J., J. E. Hill, A. M. Myers, and A. Tzagoloff.** 1991. High-expression vectors with multiple cloning sites for construction of trpE fusion genes: pATH vectors. Methods Enzymol. **194:**477–490.
28. **Krijnse-Locker, J., S. Schleich, D. Rodriguez, B. Goud, E. J. Snijder, and G. Griffiths.** 1996. The role of a 21-kDa viral membrane protein in the assembly of vaccinia virus from the intermediate compartment. J. Biol. Chem. **271:**14950–14958.
29. **Lin, C.-L., C.-S. Chung, H. G. Heine, and W. Chang.** 2000. Vaccinia virus envelope H3L protein binds to cell surface heparan sulfate and is important for intracellular mature virion morphogenesis and virus infection in vitro and in vivo. J. Virol. **74:**3353–3365.
30. **McDonald, W. F., V. Crozel-Goudot, and P. Traktman.** 1992. Transient expression of the vaccinia virus DNA polymerase is an intrinsic feature of the early phase of infection and is unlinked to DNA replication and late gene expression. J. Virol. **66:**534–547.
31. **Mercer, J., and A. Helenius.** 2008. Vaccinia virus uses macropinocytosis and apoptotic mimicry to enter host cells. Science **320:**531–535.
32. **Mercer, J., and P. Traktman.** 2003. Investigation of structural and functional motifs within the vaccinia virus A14 phosphoprotein, an essential component of the virion membrane. J. Virol. **77:**8857–8871.
33. **Moss, B.** 2006. Poxvirus entry and membrane fusion. Virology **344:**48–54.
34. **Moss, B., E. N. Rosenblum, E. Katz, and P. M. Grimley.** 1969. Rifampicin: a specific inhibitor of vaccinia virus assembly. Nature **224:**1280–1284.
35. **Nelson, G. E., T. R. Wagenaar, and B. Moss.** 2008. A conserved sequence within the H2 subunit of the vaccinia virus entry/fusion complex is important for interaction with the A28 subunit and infectivity. J. Virol. **82:**6244–6250.
36. **Ojeda, S., A. Domi, and B. Moss.** 2006. Vaccinia virus G9 protein is an essential component of the poxvirus entry-fusion complex. J. Virol. **80:**9822–9830.
37. **Ojeda, S., T. G. Senkevich, and B. Moss.** 2006. Entry of vaccinia virus and cell-cell fusion require a highly conserved cysteine-rich membrane protein encoded by the A16L gene. J. Virol. **80:**51–61.
38. **Punjabi, A., K. Boyle, J. DeMasi, O. Grubisha, B. Unger, M. Khanna, and P. Traktman.** 2001. Clustered charge-to-alanine mutagenesis of the vaccinia virus A20 gene: temperature-sensitive mutants have a DNA-minus phenotype and are defective in the production of processive DNA polymerase activity. J. Virol. **75:**12308–12318.
39. **Punjabi, A., and P. Traktman.** 2005. Cell biological and functional characterization of the vaccinia virus F10 kinase: implications for the mechanism of virion morphogenesis. J. Virol. **79:**2171–2190.
40. **Ravanello, M. P., and D. E. Hruby.** 1994. Conditional lethal expression of the vaccinia virus L1R myristylated protein reveals a role in virion assembly. J. Virol. **68:**6401–6410.
41. **Resch, W., K. K. Hixson, R. J. Moore, M. S. Lipton, and B. Moss.** 2007. Protein composition of the vaccinia virus mature virion. Virology **358:**233–247.
42. **Rochester, S. C., and P. Traktman.** 1998. Characterization of the single-stranded DNA binding protein encoded by the vaccinia virus I3 gene. J. Virol. **72:**2917–2926.
43. **Rodriguez, D., M. Esteban, and J. R. Rodriguez.** 1995. Vaccinia virus A17L gene product is essential for an early step in virion morphogenesis. J. Virol. **69:**4640–4648.
44. **Rodriguez, D., C. Risco, J. R. Rodriguez, J. L. Carrascosa, and M. Esteban.** 1996. Inducible expression of the vaccinia virus A17L gene provides a synchronized system to monitor sorting of viral proteins during morphogenesis. J. Virol. **70:**7641–7653.
45. **Rodriguez, D., J.-R. Rodriguez, and M. Esteban.** 1993. The vaccinia virus 14-kilodalton fusion protein forms a stable complex with the processed protein encoded by the vaccinia virus A17L gene. J. Virol. **67:**3435–3440.
46. **Senkevich, T. G., and B. Moss.** 2005. Vaccinia virus H2 protein is an essential component of a complex involved in virus entry and cell-cell fusion. J. Virol. **79:**4744–4754.
47. **Senkevich, T. G., S. Ojeda, A. Townsley, G. E. Nelson, and B. Moss.** 2005. Poxvirus multiprotein entry-fusion complex. Proc. Natl. Acad. Sci. USA **102:**18572–18577.
48. **Senkevich, T. G., B. M. Ward, and B. Moss.** 2004. Vaccinia virus entry into cells is dependent on a virion surface protein encoded by the A28L gene. J. Virol. **78:**2357–2366.
49. **Smith, G. L., and M. Law.** 2004. The exit of vaccinia virus from infected cells. Virus Res. **106:**189–197.
50. **Smith, G. L., A. Vanderplasschen, and M. Law.** 2002. The formation and function of extracellular enveloped vaccinia virus. J. Gen. Virol. **83:**2915–2931.
51. **Townsley, A. C., and B. Moss.** 2007. Two distinct low-pH steps promote entry of vaccinia virus. J. Virol. **81:**8613–8620.
52. **Townsley, A. C., T. G. Senkevich, and B. Moss.** 2005. The product of the vaccinia virus L5R gene is a fourth membrane protein encoded by all poxviruses that is required for cell entry and cell-cell fusion. J. Virol. **79:**10988–10998.
53. **Townsley, A. C., T. G. Senkevich, and B. Moss.** 2005. Vaccinia virus A21 virion membrane protein is required for cell entry and fusion. J. Virol. **79:**9458–9469.
54. **Townsley, A. C., A. S. Weisberg, T. R. Wagenaar, and B. Moss.** 2006. Vaccinia virus entry into cells via a low-pH-dependent endosomal pathway. J. Virol. **80:**8899–8908.
55. **Traktman, P., and K. Boyle.** 2004. Methods for analysis of poxvirus DNA replication. Methods Mol. Biol. **269:**169–186.
56. **Traktman, P., K. Liu, J. DeMasi, R. Rollins, S. Jesty, and B. Unger.** 2000. Elucidating the essential role of the A14 phosphoprotein in vaccinia virus morphogenesis: construction and characterization of a tetracycline-inducible recombinant. J. Virol. **74:**3682–3695.
57. **Turner, P. C., B. P. Dilling, C. Prins, S. G. Cresawn, R. W. Moyer, and R. C. Condit.** 2007. Vaccinia virus temperature-sensitive mutants in the A28 gene produce non-infectious virions that bind to cells but are defective in entry. Virology **366:**62–72.
58. **Ulaeto, D., D. Grosenbach, and D. E. Hruby.** 1995. Brefeldin A inhibits vaccinia virus envelopment but does not prevent normal processing and localization of the putative envelopment receptor P37. J. Gen. Virol. **76:**103–111.
59. **Unger, B., and P. Traktman.** 2004. Vaccinia virus morphogenesis: A13 phosphoprotein is required for assembly of mature virions. J. Virol. **78:**8885–8901.
60. **Upton, C., S. Slack, A. L. Hunter, A. Ehlers, and R. L. Roper.** 2003. Poxvirus

orthologous clusters: toward defining the minimum essential poxvirus genome. J. Virol. **77:**7590–7600.
61. **Vanderplasschen, A., M. Hollinshead, and G. L. Smith.** 1998. Intracellular and extracellular vaccinia virions enter cells by different mechanisms. J. Gen. Virol. **79:**877–887.
62. **Wagenaar, T. R., and B. Moss.** 2007. Association of vaccinia virus fusion regulatory proteins with the multicomponent entry/fusion complex. J. Virol. **81:**6286–6293.
63. **Wagenaar, T. R., S. Ojeda, and B. Moss.** 2008. Vaccinia virus A56/K2 fusion regulatory protein interacts with the A16 and G9 subunits of the entry fusion complex. J. Virol. **82:**5153–5160.
64. **Wolffe, E. J., D. M. Moore, P. J. Peters, and B. Moss.** 1996. Vaccinia virus A17L open reading frame encodes an essential component of nascent viral membranes that is required to initiate morphogenesis. J. Virol. **70:**2797–2808.
65. **Yoder, J. D., T. S. Chen, C. R. Gagnier, S. Vemulapalli, C. S. Maier, and D. E. Hruby.** 2006. Pox proteomics: mass spectrometry analysis and identification of Vaccinia virion proteins. Virol. J. **3:**10.